

Recent LHCb results on CP violation in beauty decays to charmonia

Valeriia Lukashenko^{a,1,*}

^aNikhef,

Science Park 105, Amsterdam, the Netherlands

E-mail: valeriia.lukashenko@cern.ch

The latest three results from LHCb with decays of B-mesons to charmonia states are presented. The first measurement of the CP-violating phase ϕ_s in the decay with electrons $B_s^0 \rightarrow J/\psi(\rightarrow e^+e^-)\phi$ is shown. Results of an updated search of the rare decay $B^0 \rightarrow J/\psi\phi$ are given. A precise measurement of the fragmentation fraction ratio of B_s^0 and B^0 , f_s/f_d , extracted from a combination of most up-to-date LHCb results is reported.

*** The European Physical Society Conference on High Energy Physics (EPS-HEP2021), ***

*** 26-30 July 2021 ***

*** Online conference, jointly organized by Universität Hamburg and the research center DESY ***

¹For the LHCb collaboration.

*Speaker

1. Introduction

CP violation measurements are a possible key towards understanding the origin of matter-antimatter asymmetry. Beyond Standard Model effects might enhance the CP-violation levels in comparison to the Standard Model predictions. Therefore, precise measurements of the Standard Model CP-violating parameters are important parts of both testing the Standard Model and looking for possible New Physics effects. The LHCb experiment is a forward detector, which was designed specifically for the forward boosted b-mesons, and is located at Large Hadron Collider (CERN) [1]. Unique capabilities of the detector in terms of the vertex reconstruction, particle identification and mass resolution give LHCb an advantage in terms of precise measurement of CP-violation.

The following results from the LHCb collaboration are presented in these proceedings: the first measurement of the CP-violating phase ϕ_s in the $B_s^0 \rightarrow J/\psi(\rightarrow e^+e^-)\phi$ decays, search for rare $B^0 \rightarrow J/\psi\phi$ decay, and precise measurement of the f_s/f_d ratio of fragmentation fractions of B-mesons.

2. First measurement of CP-violating phase in $B_s^0 \rightarrow J/\psi(\rightarrow e^+e^-)\phi$ decays

The CP-violating ϕ_s phase appears in the interference between mixing and direct $b \rightarrow c\bar{c}s$ transitions, shown in Fig. 1. The time-dependent CP-asymmetry $A_{CP}(t)$ in such decays is approximately proportional to the $\sin(\phi_s)$,

$$A_{CP}(t) \propto \sin(\phi_s)\sin(\Delta m_s t) \quad (1)$$

where Δm_s is the mass difference between heavy and light mass eigenstates of B_s^0 meson. In the most general case, one can write the $\phi_s = -2\beta_s$ phase as,

$$\phi_s = \phi_s^{SM,tree} + \phi_s^{SM,penguin} + \Delta\phi_s^{NP} \quad (2)$$

The penguin contribution $\phi_s^{SM,penguin}$ is expected to have a small contribution to the total ϕ_s phase [2]. Therefore, any significant deviation from the SM prediction would point to a source beyond the Standard Model.

In Fig. 1 the latest HFLAV combination of the ϕ_s and $\Delta\Gamma_s$ parameters are shown, where $\Delta\Gamma_s$ is the decay width difference between the heavy and light B_s^0 states [3]. Both parameters can be

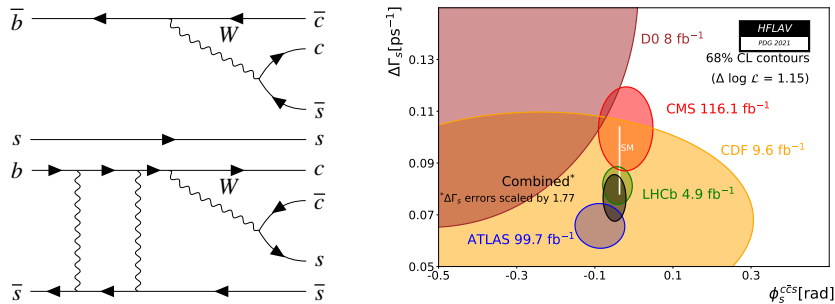


Figure 1: Direct and mixing Feynman diagrams of the $B_s^0 \rightarrow J/\psi\phi$ decay and result of the HFLAV combination of different experimental results sensitive to both ϕ_s and $\Delta\Gamma_s$ from [3].

measured in the golden decay channel $B_s^0 \rightarrow J/\psi \phi$, where $J/\psi \rightarrow \mu^+ \mu^-$ and $\phi \rightarrow K^+ K^-$ [4], [5]. As a complementary measurement one can use $B_s^0 \rightarrow J/\psi (\rightarrow e^+ e^-) \phi (\rightarrow K^+ K^-)$ decay, which is affected by different systematic uncertainty sources, but probes the same underlying physics effects as the golden decay channel [6]. In the following the $B_s^0 \rightarrow J/\psi (\rightarrow e^+ e^-) K^+ K^-$ will be referred as an electron mode and $B_s^0 \rightarrow J/\psi (\rightarrow \mu^+ \mu^-) K^+ K^-$ as a muon mode. The total data sample is $3fb^{-1}$ collected by LHCb at 7 TeV (2011) and 8 TeV (2012). The electron mode statistics corresponds to about 10% of the muon mode statistics in this sample due to the imperfect reconstruction of electrons.

Since the $B_s^0 \rightarrow J/\psi \phi$ is a pseudo-scalar particle to two vector-like particles decay, a non-trivial angular dependence of the final states has to be taken into account. It can be described by 3 polarization amplitudes: transverse parallel A_{\parallel} with angular momentum $L = 2$, transverse perpendicular A_{\perp} with $L = 1$ and longitudinal A_0 with $L = 0$. An additional amplitude A_S coming from the $B_s^0 \rightarrow J/\psi K^+ K^-$ decays without the intermediate ϕ resonance, is present in the measurement and is taken into account in the final time-dependent angular fit of the decay rate:

$$\frac{d^4\Gamma(B_s^0 \rightarrow J/\psi \phi)}{dt d\Omega} = \frac{1}{N} \sum_{k=1}^{10} f_k(\Omega) \varepsilon(t) (FT(B_s^0) \cdot h_k(t|B_s^0) + FT(\bar{B}_s^0) \cdot h_k(t|\bar{B}_s^0)) \otimes G(t|\sigma_t) \quad (3)$$

where N is a normalization factor, that includes angular acceptance weights, $f_k(\Omega)$ are the angular functions, $\varepsilon(t)$ is the decay-time acceptance, $FT(B_s^0)$ is a correction from the imperfect flavor tagging algorithms, $h_k(t|B_s^0), h_k(t|\bar{B}_s^0)$ are time evolution functions and $G(t|\sigma_t)$ is decay time resolution.

Preselection of the signal candidates is done using kinematics, particle identification and Boosted Decision Tree cuts. The purity of the sample is further improved by applying the sWeight procedure [7]. The sWeights are computed from the fit to the $m(e^+ e^- K^+ K^-)$ distribution in three categories depending on the Bremsstrahlung radiation recovery: no electrons with recovered Bremsstrahlung, one electron with recovered Bremsstrahlung and both electrons with recovered Bremsstrahlung. Time acceptance is estimated empirically from $B^0 \rightarrow J/\psi K^*$ (892) data sample and is corrected via the Monte Carlo derived weights with respect to the signal decay. Angular acceptance is determined from the Monte Carlo simulation. Flavor taggers are calibrated using $B_s^0 \rightarrow D_s^- \pi^+$ sample. Decay time resolution is floated in the fit but constrained to the decay time resolution values retrieved from the prompt muon $B_s^0 \rightarrow J/\psi K^+ K^-$ data sample, where the J/ψ and kaons are not required to have a detached vertex from the interaction point of the incoming protons. Projections of the final time-dependent angular fit (3) are shown in Fig. 2. The CP-violating phase ϕ_s is measured to be $(0.00 \pm 0.28 \pm 0.05)$ rad in the electron mode, which is consistent with the no CP-violation hypothesis. The biggest systematic sources for the electron mode come from the $m(e^+ e^- K^+ K^-)$ mass model and decay time resolution constraint.

3. Search for the rare decay $B^0 \rightarrow J/\psi \phi$

A non-resonant $B^0 \rightarrow J/\psi (\rightarrow \mu^+ \mu^-) K^+ K^-$ decay was observed in Ref. [8] with branching fraction of $(2.51 \pm 0.35 \pm 0.19) \times 10^{-6}$. A rare resonant decay $B^0 \rightarrow J/\psi \phi$ contributes to the $B^0 \rightarrow J/\psi K^+ K^-$ decay, but is suppressed by the Okubo-Zweig-Iizuka (OZI) rule [9]. According

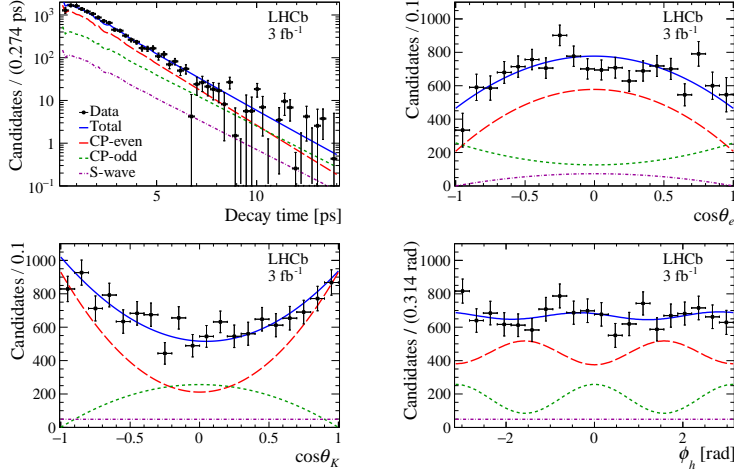


Figure 2: Results of the time-dependent angular fit projected to the four observables from [6]. The top left plot shows the projection onto the B_s^0 decay time, the top right plot onto the helicity angle between the electrons, the bottom left plot onto the helicity angles between kaons and the right bottom plot onto the angle between the decay planes of the kaons and the electrons. CP-even component includes both A_{\parallel} and A_0 amplitudes. CP-odd is A_{\perp} amplitude. A_S amplitude is called S-wave.

to the OZI rule, Feynman diagrams with disconnected quark lines are disfavored in comparison to other diagrams. The $B^0 \rightarrow J/\psi\phi$ decay is an interesting probe for the OZI rule, which was previously excluded by LHCb at $\mathcal{B}(B^0 \rightarrow J/\psi\phi) < 1.9 \cdot 10^{-6}$ with 90% CL using 2011 and 2012 data of 7 TeV and 8 TeV respectively [8]. Four production mechanisms of ϕ are possible in this decay: tri-gluon production, rescattering, photo-production and $\omega - \phi$ mixing, see Fig. 3. For an updated search a full LHCb dataset of $9fb^{-1}$, including 7 TeV, 8 TeV and 13 TeV subsets, is used [9].

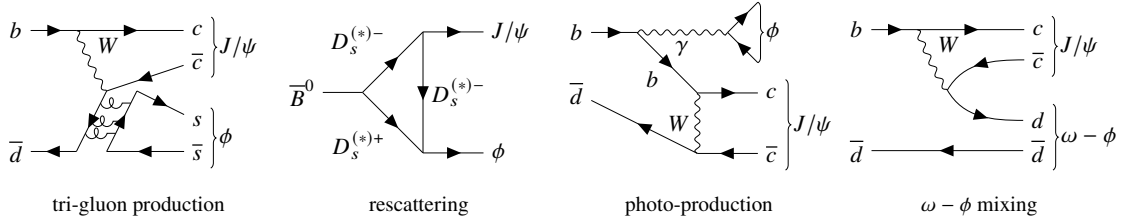


Figure 3: Four ϕ production mechanisms in the $B^0 \rightarrow J/\psi\phi$ decay. The $\omega - \phi$ mixing has the highest expected branching fraction of $O(10^{-7})$ [10].

The total number of $B^0 \rightarrow J/\psi\phi$ events N is defined as,

$$N = N_{norm} \times \frac{\mathcal{B}(B^0 \rightarrow J/\psi(\rightarrow \mu^+\mu^-)\phi)}{\mathcal{B}(B_s^0 \rightarrow J/\psi(\rightarrow \mu^+\mu^-)\phi)} \times \frac{\varepsilon_{B^0}}{\varepsilon_{B_s^0}} \times \frac{1}{f_s/f_d} \quad (4)$$

where N_{norm} is the yield of the normalization decay channel $B_s^0 \rightarrow J/\psi\phi$, \mathcal{B} are the corresponding branching fractions, ε are efficiencies and f_s, f_d are B_s^0 and B^0 fragmentation fractions. To preselect signal candidates, first the peaking background from $\Lambda_b^0 \rightarrow J/\psi pK^-$ is vetoed with kinematics cuts, after which simulation-trained Boosted Decision Tree cuts are applied together with kinematics and

particle identification cuts. A sequential mass fit is used to estimate the signal yield. The sequential mass fit procedure starts with first fitting $m(J/\psi K^+ K^-)$ for both the signal and normalization decays. In the second step the yields of $\Lambda_b^0 \rightarrow J/\psi p K^-$ events that remain in the data sample, combinatorial background and non-resonant decays extracted from the $m(J/\psi K^+ K^-)$ fit are used to fix the background yields in the $m(K^+ K^-)$ fit around the ϕ mass. This is done separately in the signal mass window with $m(J/\psi K^+ K^-)$ around the B^0 mass and normalization mass window with $m(J/\psi K^+ K^-)$ around the B_s^0 mass. Results of the sequential mass fit procedure are shown in Fig. 4. No significant signal yield is observed, and an upper limit on the branching fraction is set at the 90% CL to be $1.1 \cdot 10^{-7}$.

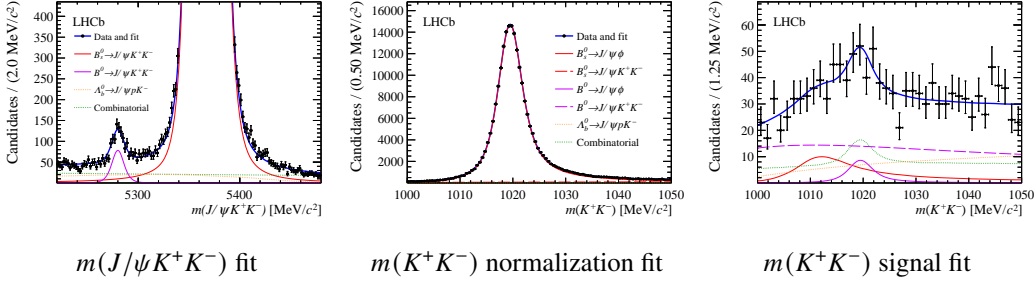


Figure 4: Results of the sequential mass fit procedure for both signal $B^0 \rightarrow J/\psi \phi$ and normalization $B_s^0 \rightarrow J/\psi \phi$ decays from [8]. Only 2015-2018, 13 TeV dataset of about $6fb^{-1}$ is shown.

4. Precise measurement of the f_s/f_d ratio of fragmentation fractions

The fragmentation fraction is a probability of a b quark to hadronize into one of the B hadrons. The ratio of the fragmentation fractions f_s/f_d is a major source of systematic uncertainty for most B_s^0 meson branching fraction measurements [11]. It has been shown that f_s/f_d depends on p_T and might have a non-negligible dependence on \sqrt{s} . In order to extract the most precise up-to-date value of f_s/f_d , multiple LHCb results are combined. The LHCb measurements that determine the ratio of efficiency-corrected yields of B_s^0 to B^+ or B^0 can be divided into three main groups: those using semileptonic final states, those using hadronic final states and those using charmonia final states. Semileptonic final states included are $B_s^0 \rightarrow D_s^- X \mu^+ \nu_\mu$, $B_s^0 \rightarrow \bar{D}^- \bar{K} X \mu^+ \nu_\mu$, $B^{+,0} \rightarrow \bar{D}^0 X \mu^+ \nu_\mu$ and $B^{+,0} \rightarrow D^- X \mu^+ \nu_\mu$. Hadronic decay modes included are $B^0 \rightarrow D^- \pi^+$, $B^0 \rightarrow D^- K^+$ and $B_s^0 \rightarrow D_s^- \pi^+$. Charmonia decay modes are $B_s^0 \rightarrow J/\psi \phi$, $B^+ \rightarrow J/\psi K^+$. In Fig. 5 one can find results of the fits to the p_T dependence of f_s/f_d from different measurements. The extracted integrated values of f_s/f_d at the three center-of-mass energies with $p_T \in [0.5, 40]$ GeV/c and $\eta \in [2., 6.4]$ are found to be: $f_s/f_d(7 \text{ TeV}) = 0.2390 \pm 0.0076$, $f_s/f_d(8 \text{ TeV}) = 0.2385 \pm 0.0075$, $f_s/f_d(13 \text{ TeV}) = 0.2539 \pm 0.0079$. Using the updated f_s/f_d value, as well as updated values of the input normalization channel branching fractions, the previous B_s^0 branching fraction measurements are updated. Using \mathcal{F}_R , the ratio of the branching fractions of $B_s^0 \rightarrow J/\psi \phi$ and $B^+ \rightarrow J/\psi K^+$, $\mathcal{B}(B_s^0 \rightarrow J/\psi \phi)$ is measured to be $(1.018 \pm 0.032 \pm 0.037) \cdot 10^{-3}$. $\mathcal{B}(B_s^0 \rightarrow D_s^- \pi^+)$, determined using data driven inputs instead of the theory inputs, is found to be $(3.20 \pm 0.10 \pm 0.16) \cdot 10^{-3}$.

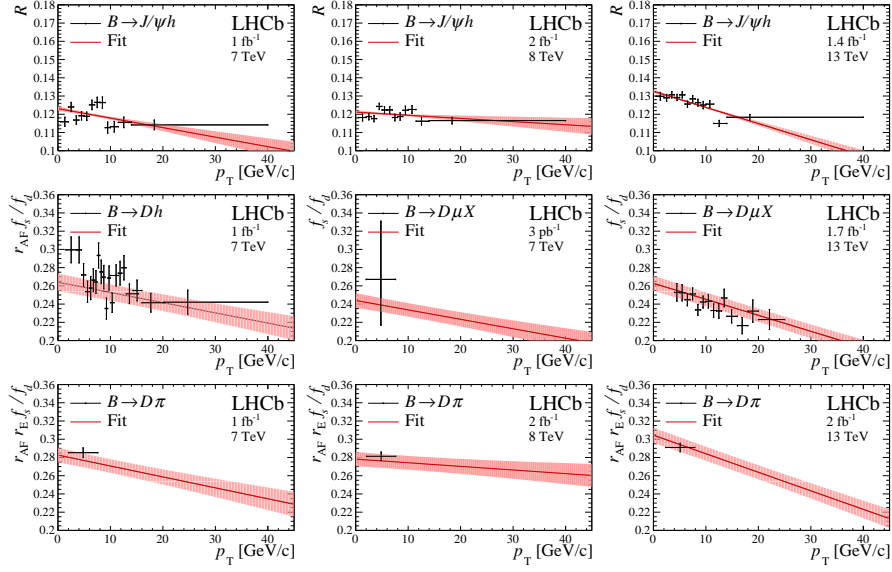


Figure 5: f_s/f_d as a function of the B-meson p_T for different measurement sets from [11]. R is the efficiency corrected yield given by $R = \mathcal{F}_R \cdot f_s/f_d$, where \mathcal{F}_R is defined in the text. r_{AF} and r_E are scale factors related to the theoretical inputs to hadronic and exchange diagrams. The fit model is defined per center-of-mass energy as $f_s/f_d(p_T, \sqrt{s}) = a_i + b_i \cdot p_T$ where $i = 7 \text{ TeV}, 8 \text{ TeV}, 13 \text{ TeV}$.

References

- [1] A. Alves and et al. *Journal of Instrumentation* **3** (2008) S08005.
- [2] R. Aaij and et al. *Physics Letters B* **742** (2015) 38–49.
- [3] Y. Amhis and et al. *The European Physical Journal C* **81** (2021) 226.
- [4] R. Aaij and et al. *Physical Review Letters* **114** (2015) .
- [5] R. Aaij and et al. *The European Physical Journal C* **79** (2019) .
- [6] R. Aaij and et al. 2105.14738.
- [7] M. Pivk and F. Le Diberder *Nucl. Instrum. Methods Phys. Res. A* **555** (2005) 356–369.
- [8] R. Aaij and et al. *Physical Review D* **88** (2013) .
- [9] R. Aaij and et al. *Chinese Physics C* **45** (2021) 043001.
- [10] M. Gronau and J.L. Rosner *Physics Letters B* **666** (2008) 185–188.
- [11] R. Aaij and et al. *Physical Review D* **104** (2021) .